

Rx3 and Shh direct anisotropic growth and specification in the zebrafish tuberal/anterior hypothalamus

Victor Muthu^{1,2}, Helen Eachus^{1‡}, Pam Ellis^{1‡}, Sarah Brown and Marysia Placzek^{1,*}

¹ The Bateson Centre and

Department of Biomedical Science, University of Sheffield,
S10 2TN, UK

² Department of Genetics, University of Pennsylvania, Philadelphia, PA 19104,
USA.

*Author for correspondence (m.placzek@sheffield.ac.uk)

‡ Equal contribution

Abstract

In the developing brain, growth and differentiation are intimately linked. Here we show that in the zebrafish embryo, the homeodomain transcription factor *rx3* co-ordinates these processes to build the tuberal/anterior hypothalamus. Analysis of *rx3 chk* mutant/*rx3* morphant fish and EdU pulse-chase studies reveal that *rx3* is required to select tuberal/anterior hypothalamic progenitors and to orchestrate their anisotropic growth. In the absence of *rx3* function, progenitors accumulate in the 3rd ventricular wall, die or are inappropriately-specified, the *shh+* anterior recess does not form, and its resident *pomc+*, *ff1b+* and *otp+ TH+* cells fail to differentiate. Manipulation of Shh signalling shows that *shh* co-ordinates progenitor cell selection and behaviour by acting as an on-off switch for *rx3*. Together our studies show that *shh* and *rx3* govern formation of a distinct progenitor domain that elaborates pattern through its anisotropic growth and differentiation.

Introduction

The hypothalamus is an ancient part of the ventral forebrain. It centrally regulates homeostatic processes that are essential to survival and species propagation, including autonomic regulation of energy balance, growth, stress and reproduction. Such adaptive functions are dependent upon the integrated function of evolutionarily-conserved neurons (reviewed in Bedont et al., 2015; Biran et al., 2015, Burbridge et al., 2016; Lohr and Hammerschmidt, 2011; Machluf et al., 2011; Pearson and Placzek, 2013; Puelles et al., 2012) that in mouse, are located within defined nuclei, including the Arc and VMN of the tuberal hypothalamus, and the PVN of the anterior hypothalamus. In zebrafish, functionally-analogous neurons exist in the periventricular tuberal (pevTub) hypothalamus and the neurosecretory preoptic (NPO) area (Biran et al., 2015; Herget et al., 2014; see Materials and Methods and Discussion for terminology). Many transcription factors and signalling ligands that govern differentiation of hypothalamic neurons from progenitor cells, likewise, have been largely conserved (reviewed in Bedont et al., 2015; Biran et al., 2015; Burbridge et al., 2016; Pearson and Placzek, 2013; Puelles et al., 2012).

The mechanisms through which secreted signalling ligands and transcription factors define and build hypothalamic territories and cells remain enigmatic (see Bedont et al., 2015; Puelles et al., 2012; Pearson and Placzek 2013). Models based on the uniform growth and differentiation of patterned territories do not account for the complex spatial patterns, or the protracted period of neuronal differentiation in the hypothalamus and at present, little is known about how early patterning events are elaborated over time. In the hypothalamus, distinct neural progenitor domains that form around the 3rd (diencephalic) ventricle (3V) are not as well-characterised as are those in other regions of the CNS. Moreover, the 3rd ventricle is sculpted into the infundibular, optic, and other smaller and ill-defined recesses in mammals (Amat et al., 1992; O'Rahilly and Muller, 1990) and lateral (LR), posterior (PR) and anterior (AR) recesses in zebrafish (Wang et al., 2009; Wang et al., 2012). Three unexplored questions are when such hypothalamic recesses form, whether they are composed of distinct progenitor

cells and whether their appearance correlates with the emergence of particular neuronal subsets.

The *Rx* paired-like homeodomain transcription factor and its fish orthologue, *rx3* are expressed within retinal and hypothalamic progenitors (Bailey et al., 2004; Bielen and Houart 2012; Cavodeassi et al., 2014; Chuang et al., 1999; Furukawa et al., 1997; Lu et al., 2013; Mathers et al., 1997; Stigloher et al., 2006; Medina-Martinez et al., 2009; Muranishi et al., 2012; Pak et al., 2014; Zhang et al., 2000) and play a central role in eye development. Disruption of *Rx* leads to small or absent eyes in mouse (Bailey et al., 2004; Mathers et al., 1997; Medina-Martinez et al., 2009; Muranishi et al., 2012; Zhang et al., 2000) and is associated with anophthalmia in humans (Voronina et al., 2004). In zebrafish, loss of function of *rx3*, including mutation in the zebrafish *rx3* gene (*chk* mutant) disrupts eye morphogenesis (Kennedy et al., 2004; Loosli et al., 2003; Stigloher et al., 2006): retinal progenitors are specified, but remain trapped in the lateral wall of the diencephalon, failing to undergo appropriate migration (Rembold et al., 2006) and differentiation (Stigloher et al., 2006).

In addition to its well-documented role in eye formation, *Rx/rx3* governs hypothalamic development. *Rx*-null mice show variable penetrance, but all display abnormalities in the ventral hypothalamus (Mathers et al 1997; Medina-Martinez et al, 2009; Zhang et al, 2000). Lineage-tracing studies demonstrate that *Rx+* progenitors give rise to *sf1+* VMN and *pomc+* Arc tuberal neurons, while targeted ablation of *Rx* in a subset of VMN progenitors leads to a fate switch from an *sf1+* VMN identity to a *dlx1+* DMN identity (Lu et al., 2013). These studies suggest that *Rx* functions in progenitor cells to cell-autonomously select *sf1+* VMN and *pomc+* Arc identities. In zebrafish, *chk* mutants and *rx3* morphants similarly show reduced numbers of *pevTub pomc+* neurons and, additionally decreased NPO *avp+* (formerly *vt*: arginine vasotocin) neurons (Dickmeis et al., 2007; Tessmar-Raible et al., 2007), although currently the underlying mechanism is unclear. These studies, together, raise the possibility that *Rx/rx3* plays a widespread role in the differentiation of tuberal and anterior/NPO hypothalamic neurons.

In mice, expression of the secreted signalling ligand, *Shh*, overlaps with that of *Rx* (Shimogori et al 2010) and conditional ablation of *Shh* from the anterior-basal hypothalamus results in phenotypes that resemble the loss of *Rx*, including a reduction/loss of *avp+* PVN and *pomc+* Arc neurons (Shimogori et al., 2010; Szabo et al., 2009). As yet, however, the link between *Shh* and *Rx/rx3* remains unclear and the mechanisms that operate downstream of *Shh* and *Rx/rx3* to govern hypothalamic differentiation are unresolved.

Here we analyse *rx3* and *shh* expression and function in the developing zebrafish hypothalamus. Analysis of *chk* mutant and *rx3* morphant fish, together with EdU pulse-chase experiments, show that *rx3* is required for a switch in progenitor domain identity, and for the survival and anisotropic growth of tuberal/anterior progenitors, including their progression to *rx3-shh+* AR cells and *pomc+*, *ff1b+* and *otp+* *TH+* tuberal/anterior fates. Timed delivery of cyclopamine or SAG reveals that *shh* signalling governs these processes via dual control of *rx3* expression, inducing, then downregulating it. We demonstrate that *rx3* downregulation, mediated by *shh* signalling, is an essential component of *rx3* function: failure to downregulate *rx3* leads to the failure of anisotropic growth, loss of the *shh+rx3-* AR and failure of tuberal/anterior cell differentiation. Together, our studies reveal a mechanism that elaborates early pattern around the hypothalamic ventricle by the selective growth of distinct progenitor cells.

Materials and Methods

Animals

Zebrafish were staged according to (Kimmel et al., 1995). *Ckh^{w29}* fish were kindly provided by Dr. Breandan Kennedy (University College Dublin, Ireland).

Nomenclature

We use the terms preoptic, anterior, tuberal and posterior to define the rostro-caudal domains of the hypothalamus. The region we define as anterior may overlap with the region that is conventionally termed the NPO (see Discussion).

In situ hybridisation

Single and double in situ hybridization methods were adapted from Thisse and Thisse 2008 and Lauter et al 2011 (details in supplementary methods), embryos post-fixed in 4% paraformaldehyde and visualised by Olympus Nomarski or confocal microscopy. For cryostat sectioning, embryos were re-fixed and equilibrated in 30% sucrose, and 15µm serial adjacent sections cut. n=10-40 embryos for wholemounts; n=4-6 embryos for sectioned data.

EdU analysis

Embryos were pulsed with 300mM EdU for 1hr on ice, chased for 1, 5 or 25h, then processed for cryostat sectioning and double EdU/in situ hybridisation analysis (details in supplementary methods) using the Click-iT EdU Alexa Fluor 488 Imaging Kit (Fisher Scientific).

Immunohistochemistry

Anti-phosP3 (Upstate) and anti-cleaved Caspase (Cell Signaling Technology) were used at 1:1000. Fixed embryos or sections were processed according to Liu et al., 2013 and mounted in VectaShield.

Length measurements

Length was determined through measurements of images, where in situ patterns could be detected relative to morphological landmarks (diencephalic-telencephalic junction (DTJ), optic commissure, lateral ventricle, posterior hypothalamus and adenohypophysis). For each experiment, length was normalized to the average length of age-matched sibling controls.

Cell quantitation

phosH3⁺ and EdU⁺ cell numbers were obtained through counts in serial adjacent sections through individual hypothalami using in situ patterns against morphological landmarks (above) to determine relative position. For *chk* mutants, section position was determined relative to unaffected posterior hypothalamus.

Image acquisition

DIC or fluorescence images were acquired using an Olympus BX60 with SPOT programme (Diagnostic Instruments Inc), Zeiss Confocal LSM510 Meta or Olympus Confocal. Data was processed with Adobe Photoshop CS3/Adobe Illustrator CS.

Statistical Analysis

Statistical analyses were performed using Prism 5. Each data value sampled were tested for Gaussian distribution prior to unpaired t-test by performing baseline subtraction of the two datasets and analyzed through D' Agostino and Pearson omnibus normality test.

Cyclopamine treatment

Cyclopamine (in ethanol) was used at 50uM, optimized on basis of *ptch1* downregulation (20,50,100,120uM tested). Cyclopamine or ethanol were added to dechorionated embryos, kept in the dark. **SAG treatment**

SAG (Millipore-EMD chemicals) in DMSO was used at 10μM, optimised on basis of *ptc1* upregulation (2,5,8,10uM tested). SAG or DMSO was added to dechorionated embryos in E3 medium, kept in dark.

Morpholino

0.25M *rx3* ATG (targets TSS) and 0.15mM *rx3* E212 (targets splice site) (GeneTools,LLC) (Tessmar-Raible et al., 2007) were injected into one-cell embryos and morphants selected on basis of absent eyes.

Abbreviations

AH	anterior hypothalamus
AR	anterior recess
Arc	arcuate nucleus
cTub	caudal tuberal hypothalamus
dA	dorso-anterior
DMN	dorsomedial nucleus
DTJ	diencephalic-telencephalic junction
NPO	neurosecretory preoptic (anterior) area
oc	optic commissure
pevTub	periventricular tuberal
PO	preoptic hypothalamus
PH	posterior hypothalamus
PR	posterior recess
PVN	paraventricular nucleus
rTub	rostral tuberal hypothalamus
SON	supraoptic nucleus
TH	tuberal hypothalamus
VMN	ventromedial nucleus
vT	ventral tuberal
zli	zone limitans intrathalamica
3V	3 rd ventricle

Results

***rx3* expression in 3rd ventricle cells**

Previous studies have described zebrafish *rx3* expression (Bielen and Houart 2012; Cavodeassi et al., 2014; Chuang et al., 1999; Kennedy et al., 2004; Loosli et al., 2003; Stigloher et al., 2006) but have not performed a detailed analysis in the 2-3 day embryo. Neurons in the hypothalamus, including *pomc+* and *avp+* neurons that are decreased/lost in the absence of *rx3* (Dickmeis et al., 2007; Tessmar-Raible et al., 2007) begin to differentiate over 2-3 days (Liu et al., 2003; Dickmeis et al., 2007; Tessmar-Raible et al., 2007) and we therefore focused on this period. At 55hpf, *rx3* is detected in three adjacent zones in the hypothalamus (Fig.1A-B"). In keeping with mouse nomenclature (Lu et al, 2013) we term these zones I, II, III, characterized by the thin strip of *rx3*^(weak+) cells in zone II. In zone I, *rx3* is expressed in neuroepithelial-like cells that form a T-shape, comprising the AR and LR of the 3rd ventricle (Fig.1B'-D') but is excluded from the AR tips (Fig.1C'D' arrowheads). In zone II, *rx3* labels cells that closely line the AR/LR, again excluded from the AR tips (Fig.1E,E', arrowheads). In zone III, *rx3* marks neuroepithelial-like cells around the 3rd ventricle which in this region (between anterior and posterior recesses, see Fig.1A,B") is small (Fig.1F,F'). At 30hpf, the entire 3rd ventricle is small and lined throughout by *rx3*⁺ neuroepithelial-like cells (Fig.1G-I). Thus the well-defined recesses of the 3rd ventricle, and characteristic *rx3*⁺ profiles, develop over 30-55hpf.

Tuberal/anterior hypothalamus elongates from proliferating *rx3*⁺ progenitors

To determine the position of *rx3*⁺ cells relative to other hypothalamic regions we compared expression to *emx2* and *fgf3*, which mark the posterior, ventro-tuberal and dorso-anterior hypothalamus (Herzog et al., 2004; Kapsimali et al., 2004; Liu et al., 2013; Mathieu et al., 2002) and to the adenohypophysis and DTJ, morphologically distinct landmarks. Over 30-55hpf, *rx3* expression is rostral and largely complementary to *emx2*, and sandwiched between ventro-tuberal and dorso-anterior *fgf3*⁺ cells (Fig.2A-H', schematics O), and in zone III, overlies the adenohypophysis. This suggests that throughout 30-55hpf *rx3* demarcates cells at the boundary of posterior and tuberal/anterior hypothalamus.

Prior to 30hpf *rx3* is expressed in progenitor cells (Bielen and Houart 2012; Cavadeossi et al., 2013; Loosli et al., 2003; Rembold et al., 2006; Stigloher et al., 2006) and the 3rd ventricle is known to harbour cycling cells (Bosco et al., 2013; Lee et al., 2006; Wang et al., 2009, 2012; Wulliman et al., 1999). To directly address whether 30hpf *rx3*⁺ cells proliferate, we pulsed fish with EdU, culled acutely, and analysed sections (Fig.2I,J). At 30hpf 77% EdU⁺ cells are *rx3*⁺ and the remainder immediately abut *rx3*⁺ cells (Fig.2I,I'; n=110 cells, 4 embryos). Co-analysis of alternate sections with EdU and phosH3 shows that S-phase cells progress to M-phase (Fig.2J,J'). Analysis of control embryos with phosH3 and *rx3* confirms that the majority of cycling cells at 30hpf are *rx3*⁺ (68% phosH3⁺ cells co-express *rx3*; 32% phosH3⁺ cells abut *rx3*⁺ cells; Figs.2K,N; n=76 cells, 4 embryos). Wholemout views of embryos double-labelled with *rx3* and phosH3 suggests that by 55hpf, fewer cycling cells are *rx3*⁺ (Fig.2L,L'). Sections confirm this, showing that at 55hpf, 35% cycling cells are *rx3*⁺, 28% abut *rx3*⁺ cells but 38% are now detected in the *rx3*⁻ recess tips (Fig 2M,N; n=92 cells, 4 embryos).

Although expressed in proliferating cells, the length of *rx3* in zones I and III does not change over 30-55hpf (Fig.2A,E) indicating its dynamic regulation. Proliferation correlates, though, with rostro-caudal growth of the tuberal/anterior hypothalamus (Figs.2A,E,O,P). Growth is greatest over 30-48hpf (Fig.1P), and is 2.5-fold greater than rostro-caudal growth of the posterior hypothalamus, or the dorsal diencephalon over this period (Fig.2Q). In summary, the tuberal/anterior hypothalamus shows anisotropic growth over 30-55hpf, driven from proliferating *rx3*⁺ cells and their immediate neighbours.

Development of *rx3-shh*⁺ AR and tuberal/anterior immature neurons

We next characterized the growing tuberal/anterior hypothalamus. At 30hpf, *shh* is detected uniformly in the hypothalamus (Fig.3A,A'): double-FISH analysis reveals extensive co-expression with *rx3* (Fig.3D,D', yellow arrowheads). *rx3+shh*⁺ cells are bounded rostrally and ventrally by *rx3+shh*⁻ cells (Fig.3D'red arrowheads) and caudally/dorsally by *shh*⁺ cells (Fig.3D' green arrowheads). In

the co-expressing region, *rx3* is strongest dorso-caudally (Fig.3D'). Similar expression domains are detected at 55hpf (Fig.3B,E) but a *shh+rx3-* domain now projects in the tuberal/anterior hypothalamus (Fig.3B,E,F,F' white arrowheads). This domain appears to be composed of cells that have downregulated *rx3*, resulting in the characteristic zone II, but is significantly (1.5-fold) longer at 55hpf compared to 30hpf (Fig.3D,E white arrows). Analysis of sections shows that *shh+rx3-* cells line the AR tips (Fig.3F' arrowheads; Supp.Fig.1A,A',C red arrowheads). Together with our previous data, this suggests that AR tip cells are *shh+/rx3-* progenitors that derive from adjacent *rx3+shh+* progenitors.

In zebrafish, immature tuberal/anterior hypothalamic neurons can be characterized through expression of the transcription factor *otpa* (Eaton and Glasgow, 2007; Lohr et al., 2009; Herget et al., 2014; Manoli and Driever, 2014), the nuclear receptor *nr5a1/sf1* orthologue, *ff1b* (Kuo et al., 2005) and the precursor polypeptide *pomc* (Liu et al., 2003; Herzog et al., 2004; Dickmeis et al., 2007; Tessmar-Raible et al., 2007; Manoli and Driever, 2014). At 30hpf *otpa* is detected in the posterior hypothalamus and at the DTJ (Fig.3G,G') but by 55hpf, additional *otpa+* cells are detected in the tuberal and anterior hypothalamus (Fig.3H,H' white arrowheads; see Eaton and Glasgow, 2007) adjacent to the *shh+* AR (Fig.3I). Ventral views show that these are periventricular, suggesting they are immature neurons (see Fig.4F; Herget et al., 2014). *ff1b* expression is detected at 30hpf (Fig.3J,J') and by 55hpf, is expressed broadly in the tuberal hypothalamus. Sections reveal that *ff1b* is expressed in *shh+* AR cells and adjacent periventricular cells (Fig.3K-K"). *pomc+* cells cannot be detected in the 30hpf hypothalamus (Fig.3L,L') but by 55hpf are detected in the tuberal hypothalamus (Fig.3M-M") rostral to *rx3+* progenitors (Fig.3N white arrowheads). Together, our data show that anterior elongation correlates with the development and growth of a *shh+rx3-* AR and with the differentiation of *otp+*, *ff1b+* and *pomc+* cells in the tuberal/anterior hypothalamus (schematized in Fig.3O,P).

rx3 is required for *shh*+ AR and neuronal differentiation

We next addressed the requirement for rx3 in development of the tuberal/anterior hypothalamus. Previous studies have shown that *pomc*+ and *avp*+ neurons are absent in embryos lacking rx3 (Dickmeis et al., 2007; Tessmar-Raible et al 2007) but a more extensive characterization of other progenitor/differentiating cells has not yet been performed.

Analysis of 55hpf *ckh* embryos shows that the *shh*+ AR fails to develop in *ckh* mutants (Fig.4A-B", white asterisk; note that posterior *shh* expression in the floor plate and basal plate appears unaltered). *rx3* expression itself is markedly different in *ckh* mutant embryos compared to siblings: zones I-III cannot be clearly resolved, (Fig.4A',B',G-H").

The failure in development of the *shh*+ AR correlates with a failure in differentiation. Mutant embryos lack *otp*+ cells in both the tuberal and anterior hypothalamus (Fig.4C-D" white arrowheads: note *otp*+ cells in the posterior hypothalamus and at the DTJ (green arrowheads) appear unaffected). Previous studies suggest that the anterior *otp*+ progenitors give rise to Group 2/3 *tyrosine hydroxylase* (*th*)+ dopaminergic neurons (Lohr et al., 2009), and in keeping with this, mutant embryos lack Group 2/3 *th*+ neurons (Fig.4E-F" white arrowheads: note Group 4-6 *th*+ neurons are not eliminated). *rx3* mutant embryos additionally lack *pomc*+ cells (Fig.4I-J" white arrowheads) and *ff1b*+ cells (Fig.4K-L", white arrowheads) in the tuberal hypothalamus (note *pomc*+ cells in the adenohypophysis (green arrowheads) are still detected) Finally, *fezf1*, a HD gene that in mouse is regulated by *sf1* (Kurrasch et al 2007) and in fish, regulates *otpb* (Blechman et al., 2007), is markedly reduced (Fig.4M-N" white arrowheads); at the same time, ectopic expression is detected in the telencephalon. *rx3* morphant embryos closely phenocopy *ckh* mutants (SuppFigs.2,3; Fig.6F-I, Fig.7). Together, these analyses show that rx3 is required for establishment of the *shh*+*rx3*- AR and for the differentiation of tuberal/anterior cells (Fig.4O,P).

Rx3 represses dorsal and ventro-tuberal progenitors

We postulated that, as in mouse (Lu et al 2013), *rx3* may switch the identity of other progenitor domains to select posterior tuberal/anterior progenitor fates, and that the absence of *rx3* will lead to alterations in progenitor domains/increased alternate fates.

The transcription factor *nkx2.1* (previously known as *nkx2.1a* (Manoli and Driever, 2014)), whose homologue in mouse is required for tuberal neuronal differentiation (Correa et al., 2015; Kimura et al., 1996; Yee et al., 2009), shows subtle difference in expression in *ckh* mutants at 25hpf: two sets of *nkx2.1+* cells in the forming tuberal/anterior hypothalamus (Fig.5A,A' blue arrowheads) cannot be detected (Fig.5B,B'). By 55hpf, this difference is pronounced: *nkx2.1* is reduced in the anterior hypothalamus and not detected in the rostral tuberal hypothalamus (Fig.5C,D; position of tuberal/anterior hypothalamus confirmed through double-labelling with *shh* (Fig.5C',D')). *nkx2.1* in the caudal tuberal, posterior hypothalamus and posterior tuberculum is seemingly unchanged.

Nkx2.1/2.4 and *pax6* exert cross-repressive interactions in the hypothalamus (Manoli and Driever, 2014), prompting us to examine expression of *pax6*. In control embryos, *pax6* is confined to the thalamus/dorsal hypothalamus and abuts the dorsal-most boundary of *rx3* (Fig.5E,E'). In the absence of *rx3*, *pax6* is detected ectopically in the tuberal/anterior hypothalamus within and rostral to *rx3+* cells (Fig.5F red arrowheads, Supp Fig.2). Thus the absence of *rx3* leads to a ventral expansion of *pax6+* progenitors.

Ectopic *pax6+* domains do not extend throughout *rx3* zone III (Fig.5F red dotted outline) raising the question of whether other progenitors are also affected by loss of *rx3*. The ets transcription factor, *pea3*, is expressed in the hypothalamus at 30hpf, and overlaps with *rx3* zone III cells (Fig.3G,G'). *pea3* is downregulated at 55hpf in control embryos but expression persists in *ckh* mutants (Fig.3H,I). These results suggest that *rx3* normally suppresses both dorsal *pax6+* and ventro-tuberal *pea3+* progenitors and predicts a widespread change in the

profile of other progenitor markers in *chk* mutants. In support of this idea, *asc1a* and *sox3* expression do not resolve in zones I, II and III in *chk* mutant embryos, in contrast to their appearance in controls (Supp.Fig.4A-H white arrowheads).

In mouse, conditional ablation of Rx leads to a failure to select arcuate/VMN fates, and instead, additional *dlx*⁺ DMN cells form (Lu et al 2013). To determine whether the increase in *pea3*⁺ and *pax6*⁺ expression results in an increase in, respectively, ventro-tuberal and DMN-like cells, we examined the neurohypophyseal marker, *fgf3* and the DMN marker, *dlx1*. Both show slightly stronger expression in *chk* mutants (Supp.Fig4I-L) and the ventro-tuberal hypothalamus appears longer in *chk* mutants (Supp.Fig4A,C) suggesting that in the absence of *rx3*, there is some expansion of ventral-tuberal and dorsal progenitors and their derivatives.

***rx3* is required for progenitor survival and anisotropic growth**

The increase in *fgf3* and *dlx1* in *chk* mutants is, however, mild, suggesting that *rx3* may play a role other than switching progenitor fates. In sectioning embryos we had noticed an unusually disorganized accumulation of *shh*⁺ cells (Fig.6A-C,G-I) suggesting that some ectopic progenitors may accumulate in the recess walls, rather than grow and progress to normal fates.

To examine this further, we compared proliferation and fate in control and *rx3*-null embryos. Loss of *rx3* led to a significant increase in *phosH3*⁺ cells in the 55hpf embryo (Fig.6D-F,J,K) that, in contrast to controls, were largely in or adjacent to *rx3*⁺ cells (Fig.6L). To better determine the fate of proliferating progenitors, we pulsed 30hpf fish with EdU, chased to 55hpf and, on serial adjacent sections, analysed whether EdU⁺ cells progressed to periventricular cells in the tuberal/anterior hypothalamus, were retained as *rx3*⁺ or *shh*⁺ progenitors, or assumed other fates. In *chk* siblings, the majority (63%; n=156 cells, 6 embryos) EdU⁺ cells were laterally-oriented chains in the anterior (Fig.6M) or tuberal (Fig.6P) hypothalamus and were detected in/in the vicinity of *ff1b*⁺ and *pomc*⁺ cells (Fig.6M,O,P). A minority (27%) were *shh*⁺*rx3*⁻ anterior (Fig.6N,O) or lateral (not shown) recess tip cells. No EdU⁺ *rx3*⁺ cells were

detected in zones I or III (Fig.6R and not shown). By contrast, in *ckh* mutant embryos, no EdU+ cells were detected in the region rostral to the adenohypophysis, ie the regions that would form part of the anterior/tuberal hypothalamus (Fig.6T-W). The majority (76%, n=165 cells, 6 embryos) EdU-labelling was detected in/adjacent to *shh*+ (Fig.6X) *rx3*+ (Fig.6Y) cells. EdU+ cells accumulated especially at the recess junctions and tips. No cleaved (c)Caspase+ cells were detected after the 25h chase period, but after a 5h chase, cCaspase+ cells, including EdU+cCaspase+ cells were detected in *ckh* mutants (Fig.6Z). No cCaspase was detected in siblings (Fig.6S).

These findings, together with our previous observations, suggest that *rx3*+ progenitors give rise to cells, including *shh*+ AR tip cells, that grow anisotropically and give rise to anterior/tuberal cells. Additionally, these findings show that in the absence of *rx3* function, many progenitor cells accumulate in the recesses, where they either die, or fail to differentiate. Together, these observations point to a mechanism in which *rx3* selects tuberal/anterior progenitors and governs their survival and growth (Fig.6 schematics).

Shh is an 'on-off' switch for rx3

Our findings demonstrate that *rx3* is upstream of *shh* in the tuberal/anterior hypothalamus. However, given the critical role of *shh* in induction and early patterning of the hypothalamus (Bedont et al., 2014; Burbridge et al., 2016; Pearson and Placzek, 2013; Blaess et al., 2015) we wished to test whether at earlier stages of hypothalamic development, *shh* is upstream of *rx3*, a possibility suggested by the observation that at epiboly stages, *shh* is expressed on midline cells, close to the early zone of *rx3* expression (Supp.Fig.5A,B).

Ptch1, a Shh-receptor and ligand-dependent antagonist, is weakly detected in the forming tuberal/anterior hypothalamus at 30hpf (Fig.7A), but not detected when embryos are exposed to cyclopamine over 10-28hpf (Fig.7G). Similar observations were made with *ptch2* (not shown). At the same time, cyclopamine treatment results in a marked downregulation of *rx3* (Fig.7B,H) mimicking the phenotype of slow-muscle-omitted (*smu*) mutant zebrafish that lack essential

components of the Hh pathway (Supp.Fig.5C,D). Together these results suggest that shh induces *rx3* in the early embryo.

By 55 hpf, strong *ptch1* expression is detected in zones I and III (Fig.7C) and weaker expression in zone II (Fig.7C). *ptch2* expression appears similar (not shown). To determine whether shh influences *rx3* at this stage, we exposed embryos to cyclopamine over 28-55hpf. This resulted in an effective inhibition of shh signaling, as judged by *ptc1* downregulation (Fig.7I) but led to a consistent increase in *rx3* expression (Fig.7D,J). Increased *rx3* expression was accompanied by changes that appeared to phenocopy loss of *rx3*, notably a significant decrease in tuberal/anterior territory (Fig.7D,J white lines and red arrows), a decrease in hypothalamic *pomc*⁺ cells (Fig.7E,K,M), the loss of *ff1b* expression (Fig.7F,L), a decrease in th⁺ Group2/3 neurons (Supp.Fig.5E,F; note Groups 4-6 in the posterior hypothalamus are unaffected) and a failure to resolve *sox3* to zones I,II and III (not shown). These observations suggest that shh mediates *rx3* downregulation in zone II, and that this is essential for differentiation of tuberal/anterior hypothalamic progenitors.

This idea predicts that provision of shh may be sufficient to rescue the phenotypic effects of *rx3* morphant embryos, once the effects of the morpholino begin to disappear. To test this, we attempted a 'late rescue', in which *rx3* morphant embryos were exposed to the small molecule shh agonist, SAG over 28-55hpf. SAG was effective in restoring a normal pattern of shh signaling in *rx3* morphant embryos, as judged by expression of *ptch1* (Fig.7N,T). Furthermore, both the normal pattern of *nkx2.1* and the characteristic profile of *rx3* in zones I, II and III were restored (Fig.7O,P,U,V). Both *pomc*⁺ and *ff1b*⁺ cells were restored in *rx3* morphant embryos in response to SAG administration (Fig.7Q,Q',R,W,X). Finally, cellular homeostasis was restored: the enhanced numbers of phos-H3⁺ cells in *rx3* morphants were reduced to normal, wild-type levels (Fig.7S,S',Y). This rescue is not seen in an early SAG-treated regime (10-28hpf; not shown), or in *chk* mutant embryos, treated with SAG over 28-55hpf (Supp.Fig.6) indicating that functional *rx3* is required for the late rescue. Together these results suggest

that a Shh-rx3 ON and Shh-rx3 OFF feedback loop (Fig.7Z) is essential for the development of the tuberal/anterior hypothalamus.

Discussion

Here we show that *rx3* is required for morphogenesis of the tuberal/anterior hypothalamus and governs three aspects of cell behaviour: it re-specifies progenitor types to tuberal/anterior identities, promotes their survival and governs their anisotropic growth/migration. Shh co-ordinates tuberal/anterior progenitor selection and behaviour by acting as an on-off switch for *rx3*. Thus a shh-rx3 feed-forward/feedback loop generates tuberal/anterior progenitors that grow to expand the surface area of the 3rd ventricle and diversify the neuronal subtypes that differentiate around it.

rx3 selects tuberal/anterior hypothalamic progenitors

Our studies confirm that *rx3* is not required for induction or initial hypothalamic patterning (Kennedy et al., 2004), but show that it is essential to elaborate pattern. Our data suggest that *rx3* autonomously selects *nkx2.1+* tuberal/anterior progenitors that grow anisotropically. In *ckh* mutant embryos, *pax6a* expands ventrally into *rx3+* progenitors, a phenotype detected as early as 19hpf (Loosli et al., 2003). The ventral expansion of *pax6a* mimics the phenotype of *nkx2.1/nkx2.4a/nkx2.4b*-null embryos (Manoli and Driever, 2014) and suggests that *rx3* re-specifies progenitors that would otherwise assume a dorsal hypothalamic or prethalamic identity.

At the same time, *rx3* represses *pea3*. In wild type animals, *pea3* overlaps with ventral-most *rx3* at 30hpf, but is downregulated by 55hpf. In *ckh* mutant fish, *pea3* persists. Although we have not performed double FISH with *pea3* and *pax6* in *ckh* mutant fish, their expression patterns appear complementary. This suggests that *rx3* operates as a switch in at least two separate progenitor populations and provides a prosaic interpretation for the existence of two domains - the dorsal *rx3+shh+* and ventral *rx3+shh-* domains.

Our studies reveal that *rx3* promotes alternate fates in progenitor cells. Its loss leads to one of three outcomes: to undergo apoptosis or to be retained as a proliferating VZ cell (novel outcomes), or to initiate alternate adjacent differentiation programmes: after pulse-chase, some EdU+ cells are detected in periventricular regions in *ckh* mutants where it is likely that they contribute to *nkx2.1+pea3+* progenitors and hence *fgf*-expressing neurohypophysis ventrally, and to *dlx1+* cells dorsally. *Dlx1+* cells are likely to be immature DMN-like neurons and notably, *crf+* neurons persist in *ckh* mutants (Dickmeis et al., 2007). Together our studies suggest that *rx3* selects tuberal/anterior neuronal progenitors and limits both ventro-tuberal neurohypophyseal and DMN-like progenitors.

In addition to promoting cell survival, *rx3* regulates cellular homeostasis in the tuberal/anterior hypothalamus, orchestrating a balance of proliferation and differentiation. We surmise that the increased proliferation seen in the absence of *rx3* reflects changes in Wnt or FGF signalling, both of which are upregulated in *ckh* mutants (Stigloher et al 2006; Yin et al., 2014; this study). *fgf3*, in particular, normally abuts neuroepithelial-like *rx3+shh-* cells both in zones I and III and is upregulated in *rx3* mutants. Potentially, the driving force for proliferation resides in *rx3+shh-* cells in zones I and III that progress to *rx3+shh+* cells in zone II.

Previous reports have shown that *rx3* is required for retinal fate selection and that telencephalic fates are expanded in its absence (Bielen and Houart 2012; Cavadeossi et al., 2013). Our studies likewise show changes in the telencephalon/eye territory: *fezf1* is upregulated in *rx3* mutants, and both *shh* and *nkx2.1* in the telencephalon/tuberal/anterior area are greatly reduced. Together, these studies suggest that *rx3* selects fate in cells of distinct origins, anterior telencephalic and posterior diencephalic. Importantly, not all hypothalamic cells alter their identity in the absence of *rx3*: the posterior hypothalamus expresses *nkx2.1*, *shh* and *otp* as normal, the rostral-most hypothalamus expresses *otp* and *nkx2.1* and the tuberal hypothalamus expresses *nkx2.1*, *pea3* and *fgf3*, emphasising the fact that *rx3* elaborates, rather than

initiates, hypothalamic pattern.

Shh is an on-off switch for *rx3*

Our study shows that *shh* is required for both the induction of *rx3* and the progression of *rx3+* to *rx3-shh+* progenitors and demonstrates that both steps are required for tuberal/anterior hypothalamic neurogenesis. Downregulation of *shh* signalling over 10-30hpf leads to an almost complete loss of *rx3* expression. By contrast, downregulation over 30-55hpf leads to sustained *rx3* in zone II and a phenotype that is highly similar to that of *ckh* mutants: *sox3* is not downregulated, the *shh+rx3-* AR does not form, the tuberal/anterior hypothalamus is short and its resident neurons do not differentiate. Importantly, the *shh* agonist, SAG, can restore normal patterns of proliferating progenitors and neuronal differentiation in late *rx3* morphants. The most likely interpretation of these findings is that *shh*-mediated *rx3* upregulation is required to select tuberal/anterior progenitors but that *shh*-mediated *rx3* inhibition is required for these to realise their differentiation programme(s). Future studies are needed to establish whether the downregulation of *sox3*, *nkx2.1*, *ascl1* and *ptc1* that we observe in wild-type, but not *ckh* mutant fish, are similarly required for progression of tuberal/anterior progenitors. We predict that the downregulation of *ptc1*, in particular, supports *shh* active signaling from zone II cells and contributes to development of the *shh+* AR. The intricate regulation of induction and cessation of *Shh* signaling in sets of neighbouring cells is emerging as a common theme within the CNS (Briscoe and Therond, 2013) and provides the opportunity to drive expansion of territories and build increasingly complex arrays of neurons.

In summary, our studies suggest that *Shh* plays a dual role in *rx3* regulation, inducing, then repressing it, and are consistent with a model in which *shh* deriving from AR cells, feeds back to *rx3+* progenitors to promote their further differentiation.

Origins of hypothalamic neurons

Our studies show that the zebrafish tuberal hypothalamus includes regions analogous to the mouse Arc and VMN. Our EdU pulse-labelling studies suggest that *shh*⁺ AR cells and differentiating *ff1b*⁺ and *pomc*⁺ neurons derive from *rx3*⁺ cells. After a 25h chase, we detect strings of EdU⁺ cells, presumably of clonal origin, extending medio-laterally from the *shh*⁺ AR tips, to *pomc*⁺ and *ff1b*⁺ regions, favouring the idea that forming neurons derive from *rx3*⁺*shh*⁺ progenitors via *rx3*⁺*shh*⁺ progenitors. In mouse, *Rax*⁺ cells give rise to *pomc* and *sf1*⁺ neurons (Liu et al., 2013). Other mouse studies show that *Shh*⁺ hypothalamic cells give rise to tuberal neurons (Alvarez-Bolado et al., 2012), and that *Shh*-ablation in hypothalamic cells leads to the loss of *pomc* and *sf1* (Shimogori et al., 2010) and a reduction in hypothalamic territory (Alvarez-Bolado et al., 2012; Zhao et al., 2012). These studies, together with observations that loss of *Nkx2.1* results in loss of tuberal hypothalamic neurons (Correa et al., 2015; Kimura et al., 1996; Yee et al., 2009), disruptions to the infundibulum and a reduction in the size of the 3rd ventricle (Kimura et al., 1996) suggests a conserved differentiation route of *pomc* and *ff1b/sf1* immature neurons and the tuberal hypothalamus from zebrafish to mouse.

In zone I, *rx3* is expressed in the anterior hypothalamus, in a region that may be equivalent to the anterior-dorsal domain reported in mouse (Shimogori et al., 2010). Our work, together with previous studies, suggests that here, *rx3* plays a role in a conserved differentiation pathway for *Avp*⁺ and Group 2/3 *th*⁺ neurons. *Avp*⁺ and Group 2/3 *th*⁺ neurons localise within a discrete subregion of hypothalamic *otp* expression (Lohr et al., 2009; Herget et al., 2014; Herget and Ryu, 2015) and in fish, as in mouse, *otp* genes are required for AVP and TH neuronal differentiation (Acampora et al, 1999; Lohr et al., 2009; Fernandes et al, 2013). *Avp*⁺ neurons fail to differentiate in the absence of *rx3* (Tessmar-Raible et al., 2007) and we now show a specific loss of an *otpa*⁺ subset and Group 2/3 *th*⁺ neurons. This suggests that *rx3* governs a subset of *otpa*⁺ progenitors in the anterior hypothalamus that will give rise to *avp*⁺ and Group 2/3 *th*⁺ neurons. We have not yet asked whether this *otp*⁺ progenitor subset are dependent on *shh*. However, in mouse, conditional deletion of hypothalamic *shh* leads to a

reduction in *otp* expression and *Avp*⁺ neurons (Szabo et al., 2009) as well as a loss of *Sim1* in the PVN (Shimogori et al., 2010), suggesting that the *shh-rx3-shh* pathway that governs *pomc* and *ff1b* cell fate may likewise govern *Avp*⁺ and Group 2/3 *th*⁺ fates. A previous study has highlighted *Sim1* and *Otp* as core components of a conserved transcriptional network that specifies neuroendocrine as well as A11-related hypothalamic dopaminergic neurons (Lohr et al., 2009), suggesting that *rx3* may be intimately linked to this pathway. Notably, since other NPO neurons, including oxytocin⁺ (previously known as isotocin) and somatostatin⁺ neurons are not affected by loss of *rx3*, our data suggest that neurons that make up the NPO derive from discrete lineages. Our work adds to a growing body of evidence that directed cell migrations play a pivotal role in ventral forebrain/hypothalamic morphogenesis (Varga et al., 1999; Cavodeassi et al., 2014 and see Pearson and Placzek, 2013). We do not know the mechanisms that operate downstream of *rx3* to govern appropriate migration, but Eph/ephrin signalling, expression of *fgf* and *Netrin*, all of which govern cell adhesion and migration of neural cells, are disrupted in *ckh* mutant embryos (Cavadeossi et al., 2013; Yin et al., 2014; this study) and could contribute.

In conclusion, our study suggests a mechanism by which *shh* elaborates pattern in the hypothalamus. Previous reports suggest that *shh* patterns the early hypothalamus in many vertebrates, establishing early progenitor domains (reviewed in Pearson and Placzek, 2013; Blaess et al., 2012). Our study shows that in zebrafish, *shh* elaborates early pattern by switching progenitor domain identity, and promoting the survival and anisotropic growth of the new progenitor cells. Recent studies in the developing spinal cord show that the coordination of growth and specification can elaborate pattern in an expanding tissue, if molecularly distinct neural progenitor domains undergo differential rates of differentiation (Kicheva et al., 2014), raising the possibility that *shh* may govern differentiation rates in the tuberal/anterior hypothalamus. Studies in mice that reveal similarities in the phenotypes of mice in which *Shh* or *Rax* are conditionally ablated raise the possibility that features of the mechanism that we describe here may be conserved in other vertebrates.

Finally, the shh-rx3-shh loop that we describe provides a means to maintain a dynamic balance between proliferating and differentiating cells. Studies in mice show that at least a subset of *Rax+* cells persist into adulthood as stem cells (Miranda-Angulo et al., 2014) that can direct hypothalamic neurogenesis even in postnatal life. The exquisite regulation of shh, fgf and wnt signalling, via rx3, is likely to hold the key to a better understanding of hypothalamic neurogenesis throughout the lifecourse and support a better understanding of complex human pathological conditions and dysfunctional behaviours that are underlain by tuberal/anterior hypothalamic cells and circuits.

Acknowledgments

We thank Tanya Whitfield, Freek van Eeden and Vincent Cunliffe for help and advice on zebrafish experiments, and, with James Briscoe and anonymous reviewers, helpful comments. We thank Brendean Kennedy for providing *ckh* embryos and help in interrogating RNASeq data. This work was supported by the Medical Research Council of Great Britain.

Figures

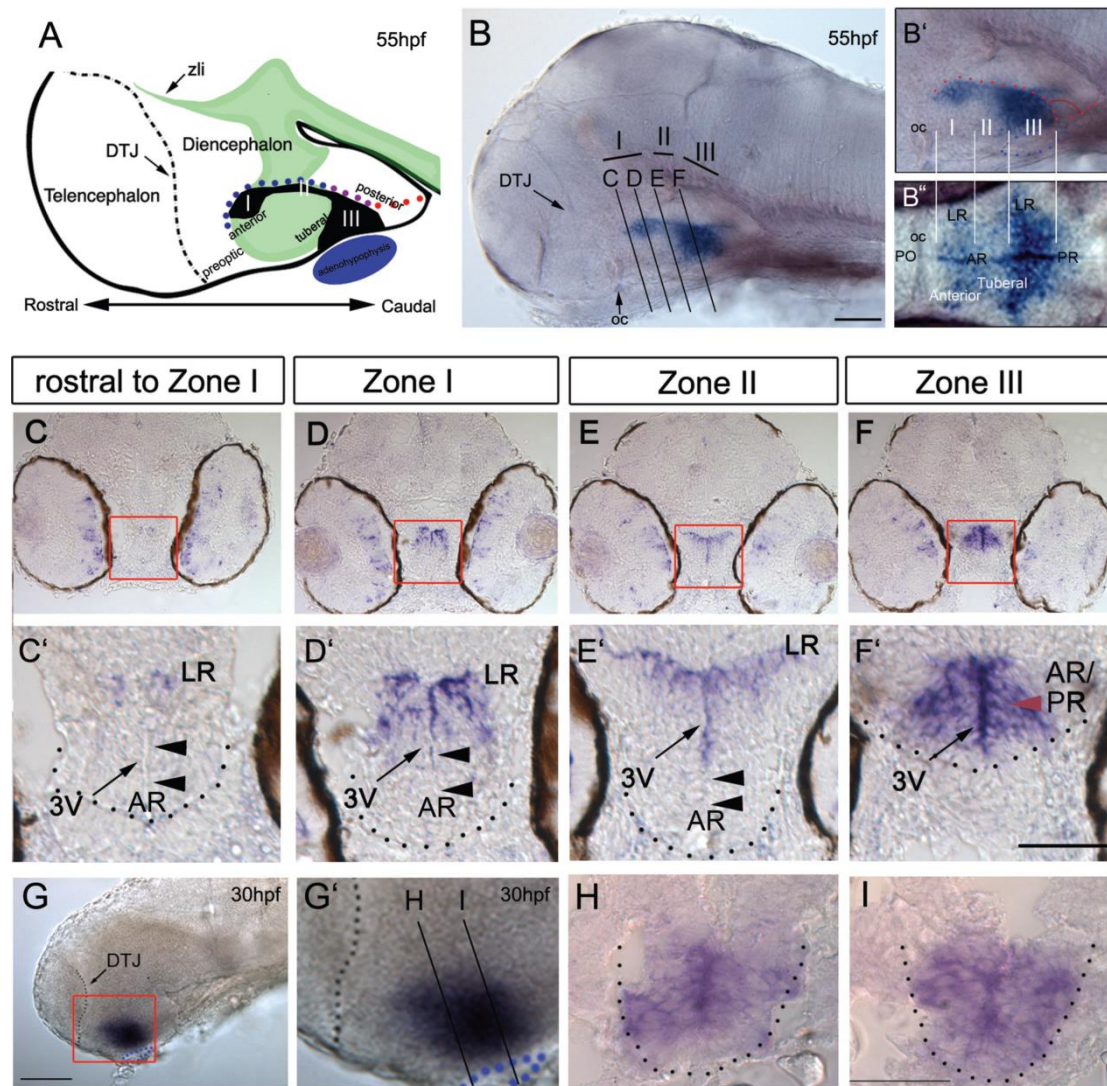


Figure 1: *rx3* expression around 3rd ventricle

(A) Schematic of 55hpf forebrain indicating subdivisions of hypothalamus relative to rostro-caudal axis and adenohypophysis (blue oval). Green and black show *shh* (Fig.3) and *rx3* expression. Dots depict rostro-caudal position of AR (blue) and PR (red) next to zone III (purple). (B-B'') Wholemount 55hpf embryo after *rx3* *in situ* hybridization. In (B) lines show planes of section in (C-F). In (B',B'') side- and ventral-views are aligned (white lines) and show position of *rx3* relative to morphological landmarks. (C-F') Representative serial sections through single embryo: bottom panels show high power views of boxed regions.

Red arrowheads point to *rx3*⁺ cells; black arrowheads point to *rx3*⁻ cells in AR tips. (G-I) Wholemount side-view of 30hpf embryo after *rx3* *in situ* hybridization; lines in (G') show positions/planes of sections in (H,I). Scale bars: 50μm

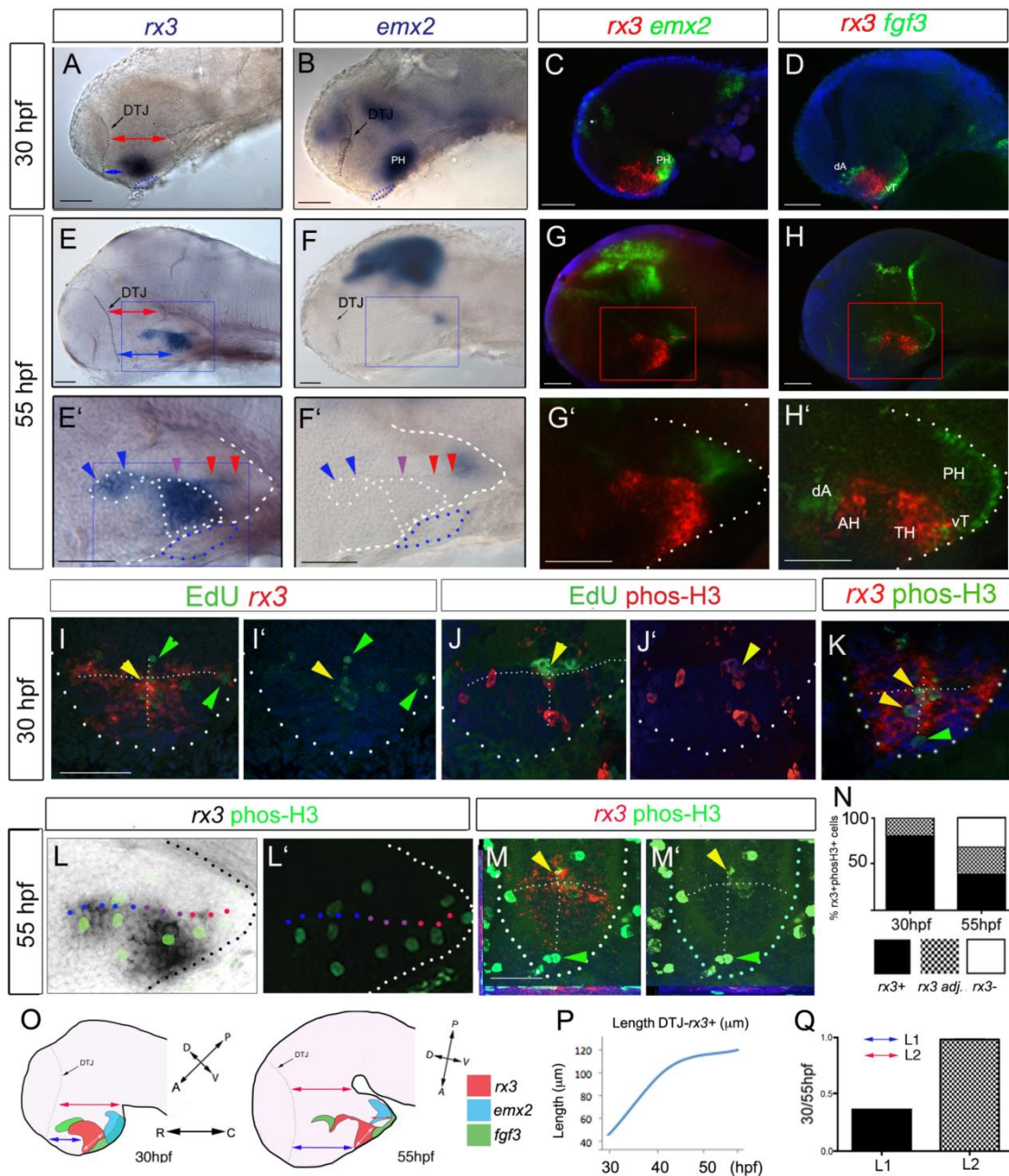


Figure 2: Anterior/tuberal hypothalamus elongates from *rx3*⁺ progenitors
 (A-H') Side views after single or double FISH at 30hpf (A-D) and 55hpf (E-H': E'-H' show high power views of boxed regions). Arrows in (A,C,E,G) show distances measured for growth comparisons. Coloured arrowheads in (E',F') indicate position of recesses. (I-K) MIP of representative sections through 30hpf embryos. (I,J) show serial adjacent sections. (I',J') show single channel views. Arrowheads show co-labelled (yellow) or single-labelled (green) cells. Small

white dotted lines indicate approximate positions of anterior and LR. (L, L') Side views of 55hpf embryo: (L') shows single channel view. (M, M') Representative single plane views taken through zone II. (M') shows single channel view. Yellow arrowheads show double-labelled cells; green arrowheads point to *phosH3+* *rx3-* cells at recess tips. (N) Quantitative analyses of cycling cells at 30-55hpf. (O) Schematic, depicting *rx3*, *fgf3* and *emx2* expression, and change in length and axial orientation of hypothalamus. A 'bending' of the tuberal/anterior hypothalamus occurs over 30-55hpf, relative to the rostro-caudal axis. Red arrows indicate length of dorsal diencephalon or length of *emx2+* PH; white arrow indicates length of ventral-most *rx3+* zone III; blue arrow indicates distance from DTJ to *rx3+* zone III. (P) Length from DTJ to rostral tip of *rx3+* zone III (n=5 embryos each at 30, 40, 48, 55hpf). (Q) Tuberal/anterior hypothalamus grows approx. 2.5-fold more than dorsal diencephalon, *emx2+* PH or ventral *rx3+* zone III (n=10 each; $p < 0.0001$). Scale bar: 50 μ m.

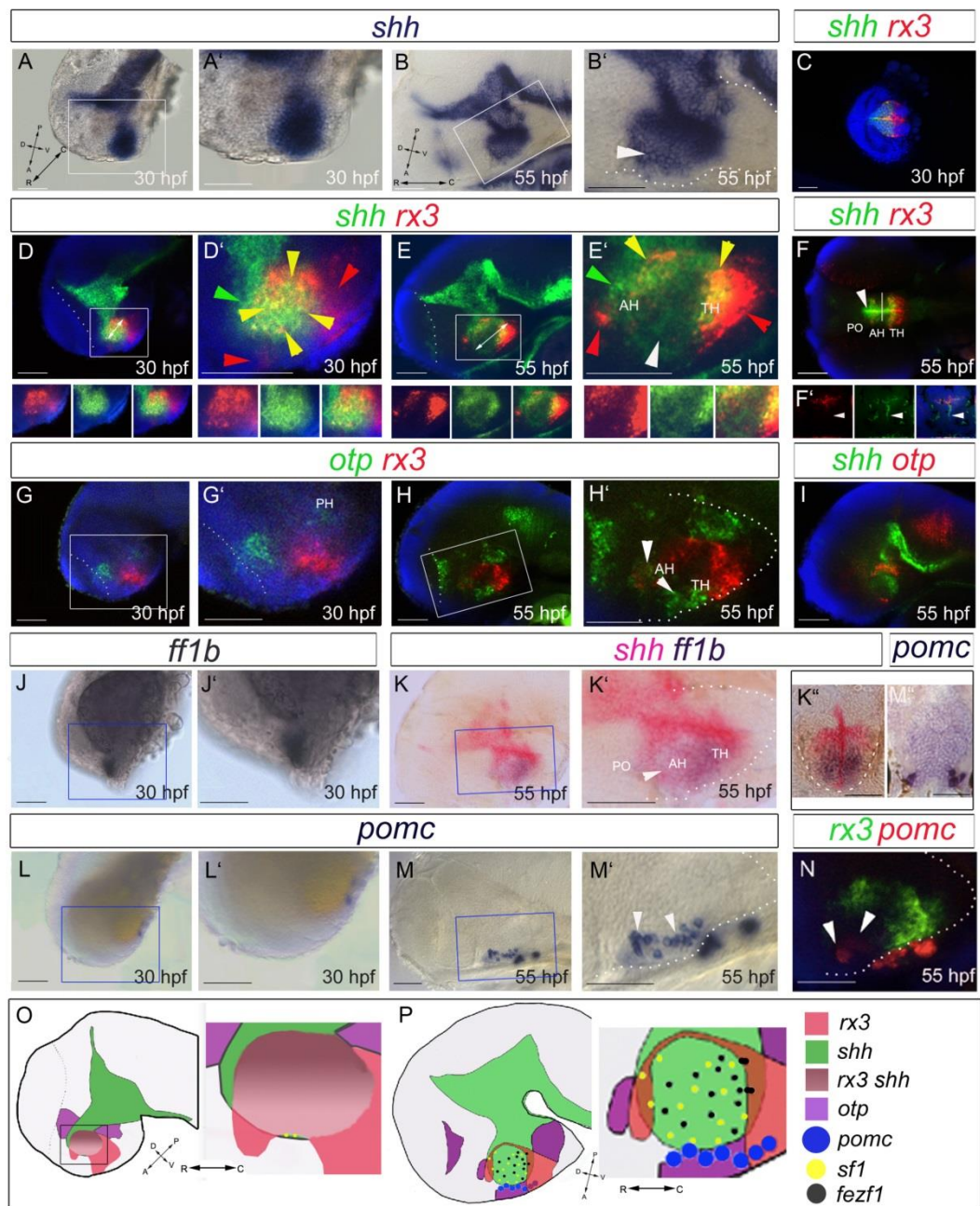


Figure 3: Differentiation in the 30-55hpf anterior/tuberal hypothalamus

Side-views (A,B,D,E,G-J,L-N), ventral-views (C,F), sagittal (K) or transverse (K',M') sections of 30hpf and 55hpf embryos. (A',B',D',E',G',H',J',L',M',N') show high power views of boxed regions. In (B',E',F) white arrowheads point to *shh*^(weak+) AR cells, in (H') to *otp*⁺ cells in the tuberal/anterior hypothalamus (H'), in (M',N) to hypothalamic *pomc*⁺ cells. In (D',E') arrowheads point to *rx3+shh*⁺ cells (yellow), *rx3*⁺ cells (red) or *shh*⁺ cells (green). (O,P) Schematics, at 30hpf (O) or 55hpf (P). Scale bars: 50µm

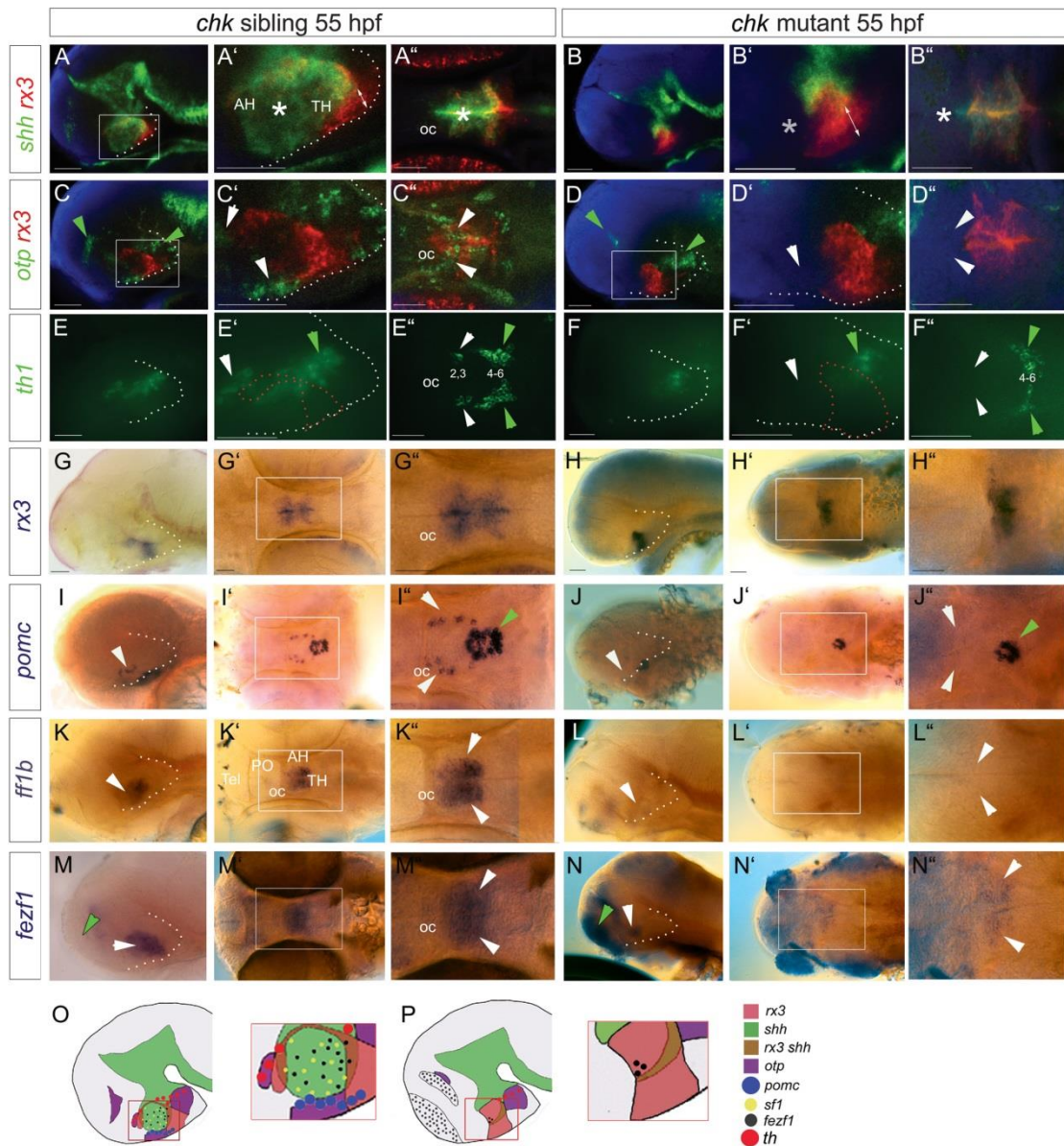


Figure 4: *rx3* is required for *shh*+ AR and anterior/tuberal differentiation

Side or ventral views of 55 hpf *chk* sibling or mutant embryos. Asterisk in (A',A'') shows *shh*+ AR, absent in *chk* mutant (asterisk, B'B''). White arrowheads point to *otp*+ tuberal/anterior cells (C',C''), Group2/3 *th*+ anterior cells (E',E''), *pomc*+ cells (I,I''), *ff1b*+ cells (K,K'') absent in *chk* mutants (D',D'',F',F'',J',J'',L,L'',N,N'') and to *fezf1*+ progenitors (M,M'') reduced in *chk* mutant (N,N''). (O,P) Schematics: boxed regions show areas shown in high power views. Scale bar: 50µm.

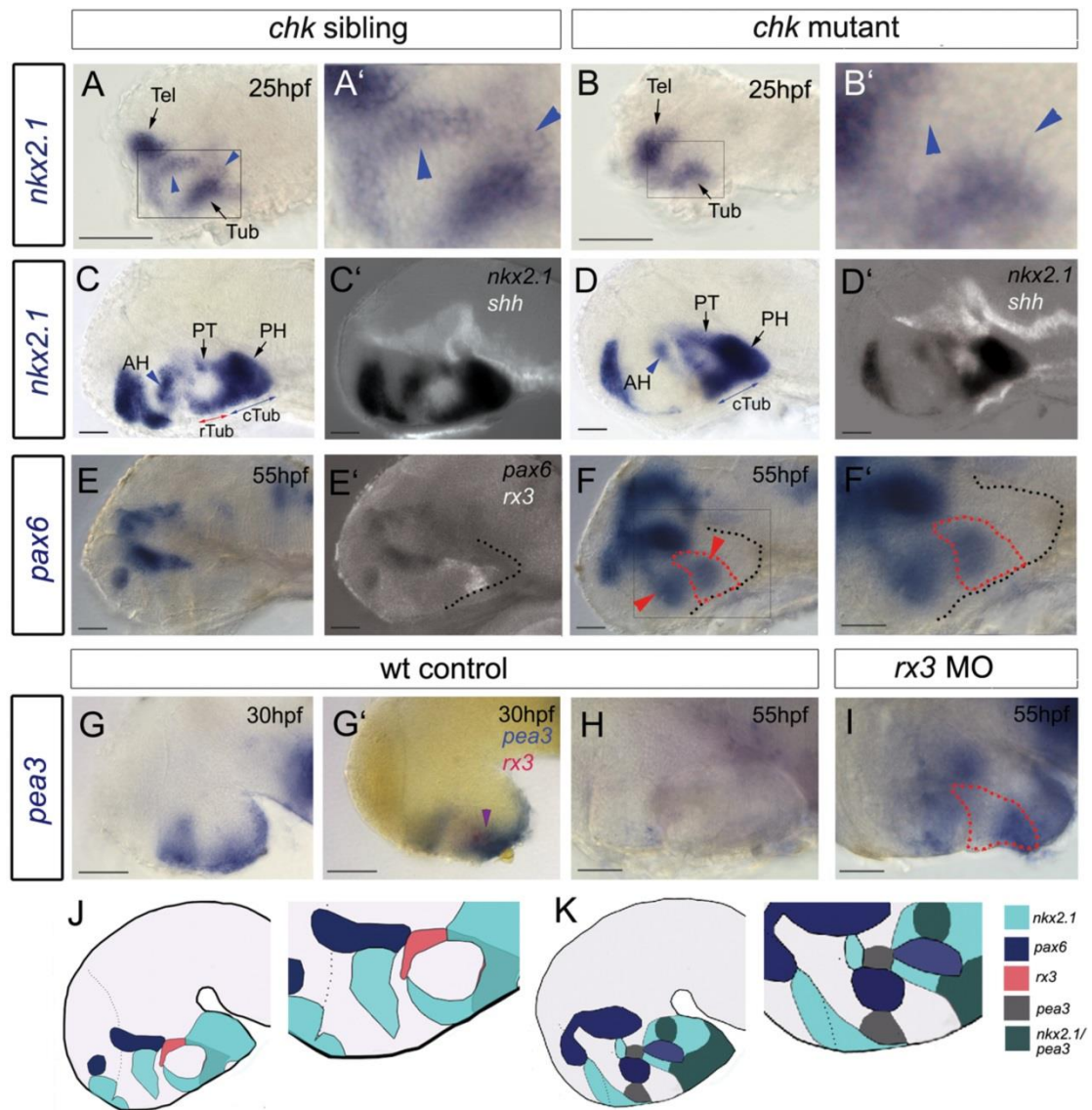


Figure 5: *rx3* suppresses dorsal and ventro-tuberal progenitors

(A-I) Side views of control or *rx3*-absent embryos. (A',B',F') show high power views of boxed regions in (A,B,F). Blue arrowheads and red arrows in (A-D) point to *nkx2.1*⁺ cells, absent in *chk* mutants. Blue arrows in (C,D) point to *nkx2.1*⁺ ventral-tuberal domain. Red arrowheads in (F) point to ectopic *pax6*⁺ cells. Red dotted outline in (F,F',I) indicates position of *rx3*⁺ cells, estimated relative to position of adenohypophysis and 3rd ventricle. Purple arrowhead in (G') points to *rx3*⁺*pea3*⁺ cells. (H,I) show views of isolated neuroectoderm. (J,K) Schematics of *chk* sibling (J) or mutant (K) 55hpf embryos. Scale bar: 50µm.

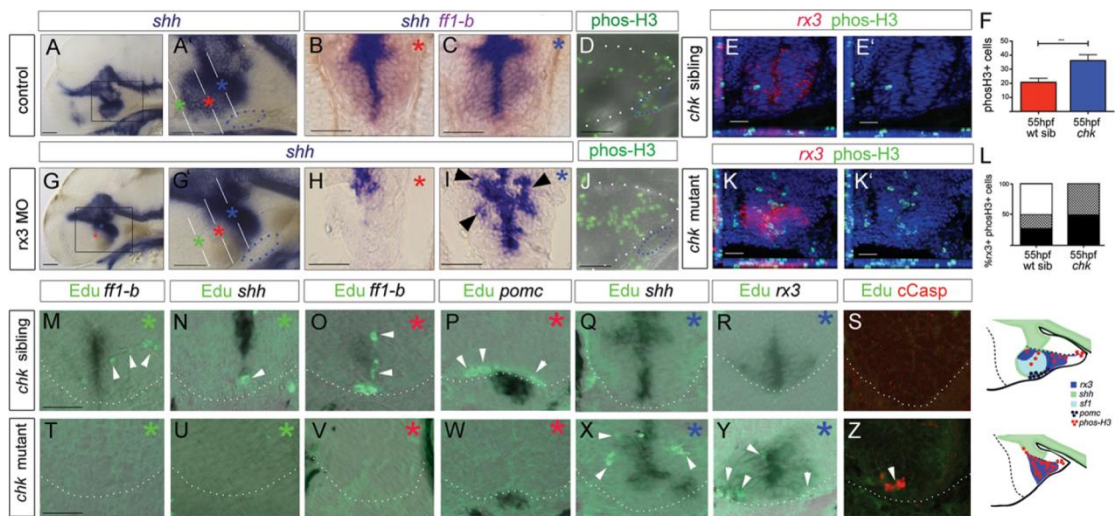


Figure 6: *rx3* promotes progenitor survival and growth

Wholemount side views (A,G) or sections (B,C,H,I: planes and positions indicated by coloured asterisks) through 55hpf embryos in control or *rx3* morphant embryos. (A',G') show high-power views of boxed regions in (A,G). Arrowheads in (I) show disorganized *shh*⁺ cells around 3V. (D,J) Wholemount side views of phosH3 in 55hpf control or *rx3* morphant embryo. (E,K) Representative sections after phosH3/*rx3* co-labelling in 55hpf *chk* sibling or mutant embryos. (E',K') show single channel views. (F,L) Quantitative analyses: (F) numbers of phosH3⁺ cells in *chk* mutant or sibling embryos (n=6 each). Significantly more phosH3⁺ cells are detected in mutants compared to siblings (p<0.001). (L) proportion of phosH3⁺ cells that are *rx3*⁺ (black), adjacent to (hatched) or distant from (white) *rx3*⁺ cells in mutant vs sibling *chk* embryos. (M-R,T-Y) Representative serial sections, from rostral-caudal (coloured asterisks denote approximate position of each section, see (A',G')) of a 55hpf *chk* sibling (M-R) or mutant (T-Y) embryos. White arrowheads point to Edu⁺ cells. (S,Z) Representative sections of a 35hpf *chk* sibling or mutant embryos. 18[±]2 cCasp⁺ cells detected in *chk* mutants, n=8 embryos. Schematics summarise mutant vs sibling *chk* embryos. Scale bar: 50µm.

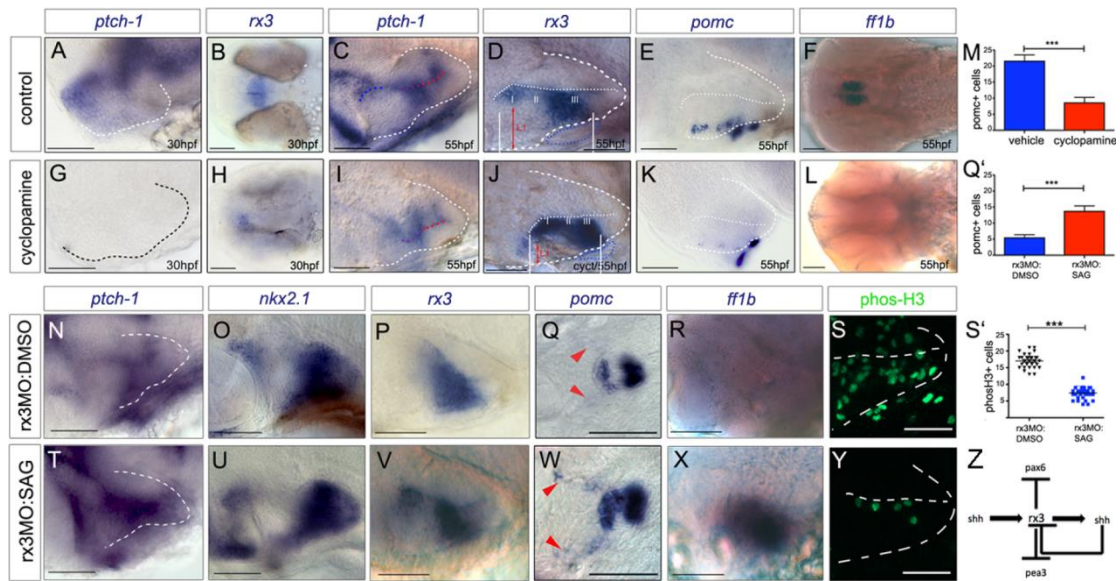


Figure 7: Shh signaling functions as an *rx3* 'on-off' switch

(A-C,F-L) Side or ventral views of 30hpf and 55hpf wild-type embryos, exposed to vehicle or cycloamine over 10-28hpf or over 28-55hpf. Red arrows and white bars in D, J show distances measured for width and length of tuberal/anterior hypothalamus. (M) Quantitative analysis: significantly fewer *pomc* cells are detected after cycloamine exposure ($p < 0.0001$, $n = 30$ embryos). (N-Y) Side or ventral views of 55hpf *rx3* morphant embryos, exposed to DMSO vehicle (N-S) or SAG (T-Y) from 28hpf. Scale bar: 50 μ m. (Z) Model for anterior/tuberal progenitor development.

References

- Acampora, D., Postiglione, M.P., Avantaggiato, V., Di Bonito, M., Vaccarino, F.M., Michaud, J., Simeone, A.** (1999). Progressive impairment of developing neuroendocrine cell lineages in the hypothalamus of mice lacking the Orthopedia gene. *Genes Dev.* **13**, 2787–2800.
- Alvarez-Bolado, G., Paul, F.A. and Blaess, S.** (2012). Sonic hedgehog lineage in the mouse hypothalamus: from progenitor domains to hypothalamic regions. *Neural Dev.* **20**; 7:4.
- Amat, P., Amat-Peral, G., Pastor, F. E., Blazquez, J. L., Pelaez, B., Alvarez-Morujó, A., Toranzo, D. and Sanchez, A.** (1992). Morphologic substrates of the ventricular route of secretion and transport of substances in the tubero-infundibular region of the hypothalamus. Ultrastructural study. *Bol Asoc Med P R* **84**, 56-66.
- Bailey, T. J., El-Hodiri, H., Zhang, L., Shah, R., Mathers, P. H. and Jamrich, M.** (2004). Regulation of vertebrate eye development by Rx genes. *Int J Dev Biol* **48**, 761-770.
- Bedont, J.L., Newman, E.A. and Blackshaw, S.** (2015). Patterning, specification and differentiation in the developing hypothalamus. *Wiley Interdiscip Rev Dev Biol.* **4**, 445-68.
- Bielen, H. and Houart, C.** (2012) BMP signaling protects telencephalic fate by repressing eye identity and its Cxcr4-dependent morphogenesis. *Dev. Cell.* **23**, 812-833.
- Biran, J., Tahor, M., Wircer, E. and Levkowitz, G.** (2015). Role of developmental factors in hypothalamic function. *Front Neuroanat.* **9**:47.
- Blaess, S., Szabó, N., Haddad-Tóvolli, R., Zhou, X. and Álvarez-Bolado, G.** (2015). Sonic hedgehog signalling in the development of the mouse hypothalamus. *Front Neuroanat.* **8**:156.
- Blechman, J., Borodovsky, N., Eisenberg, M., Nabel-Rosen, H., Grimm, J. and Levkowitz, G.** (2007). Specification of hypothalamic neurons by dual regulation of the homeodomain protein Orthopedia. *Development* **134**, 4417-4426.
- Bosco, A., Bureau, C., Affaticati, P., Gaspar, P., Bally-Cuif, L. and Lillesaar, C.** (2013). Development of hypothalamic serotonergic neurons requires Fgf signalling via the ETS-domain transcription factor Etv5b. *Development* **140**, 372-384.
- Briscoe, J. and Therond, P. P.** (2013). The mechanisms of Hedgehog signalling and its roles in development and disease. *Nat Rev Mol Cell Biol* **14**, 416-429.
- Burbridge, S., Stewart, I. and Placzek, M.** (2016). Development of the neuroendocrine hypothalamus. *J.Comp.Physiol.*
- Byerly, M. S. and Blackshaw, S.** (2009). Vertebrate retina and hypothalamus development. *Wiley Interdiscip Rev Syst Biol Med* **1**, 380-389.
- Cavodeassi, F., Ivanovitch, K. and Wilson, S.W.** (2013). Eph/Ephrin signalling maintains eye field segregation from adjacent neural plate territories during forebrain morphogenesis. *Development* **140**, 4193-4202.
- Chuang, J. C., Mathers, P. H. and Raymond, P. A.** (1999). Expression of three Rx homeobox genes in embryonic and adult zebrafish. *Mech Dev* **84**, 195-198.

- Correa, S.M., Newstrom, D.W., Warne, J.P., Flandin, P., Cheung, C., Lin-Moore, A.T., Pierce, A.A., Xu, A.W., Rubenstein, J.L. and Ingraham, H.A. (2015).** An estrogen-responsive module in the ventromedial hypothalamus selectively drives sex-specific activity in females. *Cell Rep.* **10**, 62-74.
- Dickmeis, T., Lahiri, K., Nica, G., Vallone, D., Santoriello, C., Neumann, C.J., Hammerschmidt, M. and Foulkes, N.S. (2007).** Glucocorticoids play a key role in circadian cell cycle rhythms. *PLoS Biol.* **5**, e78.
- Eaton, J.L. and Glasgow, E. (2007).** Zebrafish orthopedia (*otp*) is required for isotocin cell development. *Dev Genes Evol.* **217**, 149-58.
- Fernandes, A.M., Beddows, E., Filippi, A. and Driever, W. (2013).** Orthopedia transcription factor *otpa* and *otpb* paralogous genes function during dopaminergic and neuroendocrine cell specification in larval zebrafish. *PLoS One*, **8**, 9:e75002
- Furukawa, T., Kozak, C. A. and Cepko, C. L. (1997).** *rax*, a novel paired-type homeobox gene, shows expression in the anterior neural fold and developing retina. *Proc Natl Acad Sci U S A* **94**, 3088-3093.
- Herget, U., Wolff, A., Wullmann, M.F. and Ryu, S. (2014).** Molecular neuroanatomy and chemoarchitecture of the neurosecretory tuberal/preoptic-hypothalamic area in zebrafish larvae. *J Comp Neurol.* **522**, 1542-64.
- Herget, U. and Ryu, S. (2015).** Coexpression analysis of nine neuropeptides in the neurosecretory tuberal/preoptic area of larval zebrafish. *Front. Neuroanat.* **9**, 2.
- Herzog, W., Sonntag, C., von der Hardt, S., Roehl, H. H., Varga, Z. M. and Hammerschmidt, M. (2004).** *Fgf3* signaling from the ventral diencephalon is required for early specification and subsequent survival of the zebrafish adenohypophysis. *Development* **131**, 3681-3692.
- Kapsimali, M., Caneparo, L., Houart, C. and Wilson, S. W. (2004).** Inhibition of Wnt/Axin/beta-catenin pathway activity promotes ventral CNS midline tissue to adopt hypothalamic rather than floorplate identity. *Development* **131**, 5923-5933.
- Kennedy, B. N., Stearns, G. W., Smyth, V. A., Ramamurthy, V., van Eeden, F., Ankoudinova, I., Raible, D., Hurley, J. B. and Brockhoff, S. E. (2004).** Zebrafish *rx3* and *mab21l2* are required during eye morphogenesis. *Dev Biol* **270**, 336-349.
- Kicheva, A., Bollenbach, T., Ribeiro, A., Valle, H.P., Lovell-Badge, R., Episkopou, V and Briscoe, J. (2014).** Coordination of progenitor specification and growth in mouse and chick spinal cord. *Science* **345**, 6204:1254927.
- Kimmel, C. B., Ballard, W. W., Kimmel, S. R., Ullmann, B. and Schilling, T. F. (1995).** Stages of embryonic development of the zebrafish. *Dev Dyn* **203**, 253-310.
- Kimura, S, Hara Y, Pineau T, Fernandez-Salguero P, Fox CH, Ward JM, Gonzalez FJ. (1996).** The T/*ebp* null mouse: thyroid-specific enhancer-binding protein is essential for the organogenesis of the thyroid, lung, ventral forebrain and pituitary. *Genes Dev.* **10**, 60-9.

- Kuo, M.W., Postlethwait, J., Lee, W.C., Lou, S. W., Chan, W.K. and Chung, B.C.** (2005). Gene duplication, gene loss and evolution of expression domains in the vertebrate nuclear receptor NR5A (Ftz-F1) family. *Biochem J.* **389**, 19-26.
- Kurrasch, D.M., Cheung, C.C., Lee, F.Y., Tran, P.V., Hata, K. and Ingraham, H.A.** (2007) The neonatal ventromedial hypothalamus transcriptome reveals novel markers with spatially distinct patterning. *J Neurosci* **27**, 13624-13634.
- Langenberg, T., Kahana, A., Wszalek, J.A. and Halloran, M.C.** (2008). The eye organizes neural crest cell migration. *Dev Dyn.* **6**, 1645-1652
- Lauter, G., Soll, I., Hauptmann, G.** (2011). Multicolor fluorescent in situ hybridization to define abutting and overlapping gene expression in the embryonic zebrafish brain. *Neural Dev.* **6** doi: 10.1186/1749-8104-6-10.
- Lee, J. E., Wu, S. F., Goering, L. M. and Dorsky, R. I.** (2006). Canonical Wnt signaling through Lef1 is required for hypothalamic neurogenesis. *Development* **133**, 4451-4461.
- Liu, N.A., Hunag, H., Herzog, W. Hammerschmidt, M., Lin, S. and Melmed, S.** (2003) Pituitary corticotroph ontogeny and regulation in transgenic zebrafish. *Mol. Endocrinol.* **17**, 959-966.
- Liu, F., Pogoda, H. M., Pearson, C. A., Ohyama, K., Lohr, H., Hammerschmidt, M. and Placzek, M.** (2013). Direct and indirect roles of Fgf3 and Fgf10 in innervation and vascularisation of the vertebrate hypothalamic neurohypophysis. *Development* **140**, 1111-1122.
- Lohr, H. and Hammerschmidt, M.** (2011). Zebrafish in endocrine systems: recent advances and implications for human disease. *Annu Rev Physiol* **73**, 183-211.
- Löhr, H., Ryu, S. and Driever, W.** (2009) Zebrafish diencephalic A11-related dopaminergic neurons share a conserved transcriptional network with neuroendocrine lineages. *Development.* **136**, 1007-1017.
- Loosli, F., Staub, W., Finger-Baier, K. C., Ober, E. A., Verkade, H., Wittbrodt, J. and Baier, H.** (2003). Loss of eyes in zebrafish caused by mutation of *ckh/rx3*. *EMBO Rep* **4**, 894-899.
- Lu, F., Kar, D., Gruenig, N., Zhang, Z. W., Cousins, N., Rodgers, H. M., Swindell, E. C., Jamrich, M., Schuurmans, C., Mathers, P. H., et al.** (2013). Rax is a selector gene for mediobasal hypothalamic cell types. *J Neurosci* **33**, 259-272.
- Machluf, Y., Gutnick, A. and Levkowitz, G.** (2011). Development of the zebrafish hypothalamus. *Ann N Y Acad Sci* **1220**, 93-105.
- Manoli, M. and Driever, W.** (2014) *nkx2.1* and *nkx2.4* genes function partially redundant during development of the zebrafish hypothalamus, tuberal/preoptic region and pallidum. *Front Neuroanat.* **8**, 145.
- Mathers, P. H., Grinberg, A., Mahon, K. A. and Jamrich, M.** (1997). The Rx homeobox gene is essential for vertebrate eye development. *Nature* **387**, 603-607.
- Mathieu, J., Barth, A., Rosa, F. M., Wilson, S. W. and Peyrieras, N.** (2002). Distinct and cooperative roles for Nodal and Hedgehog signals during hypothalamic development. *Development* **129**, 3055-3065.

- Medina-Martinez, O., Amaya-Manzanares, F., Liu, C., Mendoza, M., Shah, R., Zhang, L., Behringer, R. R., Mahon, K. A. and Jamrich, M.** (2009a). Cell-autonomous requirement for rx function in the mammalian retina and posterior pituitary. *PLoS One* **4**, e4513.
- Miranda-Angulo, A. L., Byerly, M. S., Mesa, J., Wang, H. and Blackshaw, S.** (2014). Rax regulates hypothalamic tanycyte differentiation and barrier function in mice. *J Comp Neurol* **522**, 876-899.
- Muranishi, Y., Terada, K. and Furukawa, T.** (2012). An essential role for Rax in retina and neuroendocrine system development. *Dev Growth Differ* **54**, 341-348. (This is a review)
- O'Rahilly, R. and Muller, F.** (1990). Ventricular system and choroid plexuses of the human brain during the embryonic period proper. *Am J Anat* **189**, 285-302.
- Pak, T., Yoo, S., Miranda-Angulo, A. M., Wang, H. and Blackshaw, S.** (2014). Rax-CreERT2 knock-in mice: a tool for selective and conditional gene deletion in progenitor cells and radial glia of the retina and hypothalamus. *PLoS One* **9**, e90381.
- Pearson, C. A. and Placzek, M.** (2013). Development of the medial hypothalamus: forming a functional hypothalamic-neurohypophyseal interface. *Curr Top Dev Biol* **106**, 49-88.
- Puelles, L., Martinez-de-la-Torre, M., Bardet, S. and Rubenstein, J. L. R.** (2012). Hypothalamus. *Mouse Nervous System*, 221-312.
- Rembold, M., Loosli, F., Adams, R.J. and Wittbrodt, J.** (2006) Individual cell migration serves as the driving force for optic vesicle evagination. *Science* **313**, 1130-1134.
- Ronneberger, O., Liu, K., Rath, M., Ruebeta, D., Mueller, T., Skibbe, H., Drayer, B., Schmidt, T., Filippi, A., Nitschke, R., et al.** (2012). ViBE-Z: a framework for 3D virtual colocalization analysis in zebrafish larval brains. *Nat Methods* **9**, 735-742.
- Shimogori, T., Lee, D. A., Miranda-Angulo, A., Yang, Y., Wang, H., Jiang, L., Yoshida, A. C., Kataoka, A., Mashiko, H., Avetisyan, M., et al.** (2010). A genomic atlas of mouse hypothalamic development. *Nat Neurosci* **13**, 767-775.
- Stigloher, C., Ninkovic, J., Laplante, M., Geling, A., Tannhauser, B., Topp, S., Kikuta, H., Becker, T. S., Houart, C. and Bally-Cuif, L.** (2006). Segregation of telencephalic and eye-field identities inside the zebrafish forebrain territory is controlled by Rx3. *Development* **133**, 2925-2935.
- Szabo, N. E., Zhao, T., Zhou, X. and Alvarez-Bolado, G.** (2009). The role of Sonic hedgehog of neural origin in thalamic differentiation in the mouse. *J Neurosci* **29**, 2453-2466.
- Tessmar-Raible, K., Raible, F., Christodoulou, F., Guy, K., Rembold, M., Hausen, H. and Arendt, D.** (2007). Conserved sensory-neurosecretory cell types in annelid and fish forebrain: insights into hypothalamus evolution. *Cell* **129**, 1389-1400.
- Thisse, C. and Thisse, B.** (2008). High-resolution in situ hybridization to whole-mount zebrafish embryos. *Nat Protoc* **3**, 59-69.
- Varga, Z.M., Wegner, J. and Westerfield, M.** (1999). Anterior movement of ventral diencephalic precursors separates the primordial eye field in the neural plate and requires cyclops. *Development* **126**, 5533-5546.

- Voronina, V.A., Kozhemyakina, E.A., O’Kernick, C.M., Kahn, N.D., Wenger, S.L., Linberg, J.V., Schneider, A.S. and Mathers, P.H.** (2004). Mutations in the human RAX homeobox gene in a patient with anophthalmia and sclerocornea. *Hum Mol Genet.* **13**, 315-322.
- Wang, X., Kopinke, D., Lin, J., McPherson, A. D., Duncan, R. N., Otsuna, H., Moro, E., Hoshijima, K., Grunwald, D. J., Argenton, F., et al.** (2012). Wnt signaling regulates postembryonic hypothalamic progenitor differentiation. *Dev Cell* **23**, 624-636.
- Wang, X., Lee, J. E. and Dorsky, R. I.** (2009). Identification of Wnt-responsive cells in the zebrafish hypothalamus. *Zebrafish* **6**, 49-58.
- Wullmann, M.F., Puelles, L. and Wicht, H.** (1999). Early postembryonic neural development in the zebrafish: a 3-D reconstruction of forebrain proliferation zones shows their relation to prosomeres. *Eur J Morphol.* **37**, 117-121.
- Yee, C. L., Wang, Y., Anderson, S., Ekker, M. and Rubenstein, J. L.** (2009). Arcuate nucleus expression of NKX2.1 and DLX and lineages expressing these transcription factors in neuropeptide Y(+), proopiomelanocortin(+), and tyrosine hydroxylase(+) neurons in neonatal and adult mice. *J Comp Neurol* **517**, 37-50.
- Yin, J., Morrissey, M.E., Sine, L., Kennedy, C., Higgins, D.G. and Kennedy, B. N.** (2014). Genes and signaling networks regulated during zebrafish optic vesicle morphogenesis. *BMC Genomics* **15**, 825.
- Zhang, L., Mathers, P. H. and Jamrich, M.** (2000). Function of Rx, but not Pax6, is essential for the formation of retinal progenitor cells in mice. *Genesis* **28**, 135-142.
- Zhao, L., Zevallos, S.E., Rizzoti, K., Jeong, Y., Lovell-Badge, R. and Epstein, D.J.** (2012). Disruption of SoxB1-dependent Sonic hedgehog expression in the hypothalamus causes septo-optic dysplasia. *Dev Cell.* **22**, 585-96